

Inorganic-ligand exchanging time effect in PbS quantum dot solar cell

Byung-Sung Kim, John Hong, Bo Hou, Yuljae Cho, Jung Inn Sohn, SeungNam Cha, and Jong Min Kim

Citation: *Appl. Phys. Lett.* **109**, 063901 (2016); doi: 10.1063/1.4960645

View online: <https://doi.org/10.1063/1.4960645>

View Table of Contents: <http://aip.scitation.org/toc/apl/109/6>

Published by the [American Institute of Physics](#)

Articles you may be interested in

[Impact of dithiol treatment and air annealing on the conductivity, mobility, and hole density in PbS colloidal quantum dot solids](#)

Applied Physics Letters **92**, 212105 (2008); 10.1063/1.2917800

[Increasing photon absorption and stability of PbS quantum dot solar cells using a ZnO interlayer](#)

Applied Physics Letters **107**, 183901 (2015); 10.1063/1.4934946

[Single-step colloidal quantum dot films for infrared solar harvesting](#)

Applied Physics Letters **109**, 183105 (2016); 10.1063/1.4966217

[Free carrier generation and recombination in PbS quantum dot solar cells](#)

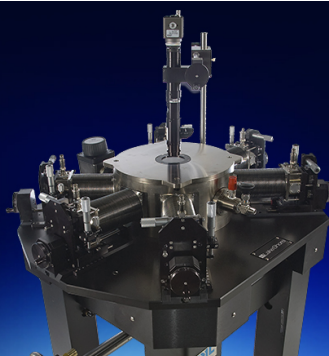
Applied Physics Letters **108**, 103102 (2016); 10.1063/1.4943379

[Detailed Balance Limit of Efficiency of p-n Junction Solar Cells](#)

Journal of Applied Physics **32**, 510 (1961); 10.1063/1.1736034

[Increased efficiency in pn-junction PbS QD solar cells via NaHS treatment of the p-type layer](#)

Applied Physics Letters **110**, 103904 (2017); 10.1063/1.4978444



Cryogenic probe stations
for accurate, repeatable
material measurements

LEARN MORE

Inorganic-ligand exchanging time effect in PbS quantum dot solar cell

Byung-Sung Kim,^{1,a)} John Hong,^{1,a)} Bo Hou,¹ Yuljae Cho,¹ Jung Inn Sohn,^{1,b)} SeungNam Cha,^{1,b)} and Jong Min Kim²

¹Department of Engineering Science, University of Oxford, Parks Road, Oxford OX1 3PJ, United Kingdom

²Department of Engineering, University of Cambridge, 9 JJ Thomson Avenue, Cambridge CB3 0FA, United Kingdom

(Received 23 May 2016; accepted 28 July 2016; published online 9 August 2016)

We investigate time-dependent inorganic ligand exchanging effect and photovoltaic performance of lead sulfide (PbS) nanocrystal films. With optimal processing time, volume shrinkage induced by residual oleic acid of the PbS colloidal quantum dot (CQD) was minimized and a crack-free film was obtained with improved flatness. Furthermore, sufficient surface passivation significantly increased the packing density by replacing from long oleic acid to a short iodide molecule. It thus facilitates exciton dissociation via enhanced charge carrier transport in PbS CQD films, resulting in the improved power conversion efficiency from 3.39% to 6.62%. We also found that excess iodine ions on the PbS surface rather hinder high photovoltaic performance of the CQD solar cell. © 2016 Author(s). All article content, except where otherwise noted, is licensed under a Creative Commons Attribution (CC BY) license (<http://creativecommons.org/licenses/by/4.0/>). [<http://dx.doi.org/10.1063/1.4960645>]

Colloidal quantum dots (CQDs) are promising candidates for next-generation photovoltaics owing to their unique properties such as high absorption coefficient, tunable band gap, and multiple exciton generation effect.^{1–4} The solution-based process also has provided high feasibility of realizing flexible and large scale photovoltaic devices with cost-effective fabrication.^{5–8} Despite these favorable characteristics, poor charge transport and imperfect surface status of CQDs hinder high photovoltaic performance compared to the theoretical conversion efficiency. During the synthetic process, CQDs are capped by long and bulky organic ligands which enable to control the size of CQDs by preventing over-size aggregation and enhancing chemical stability.⁹ However, the insulating properties of long hydrocarbon ligands limited photoexcited carrier transport, eventually resulting in low power conversion efficiency (PCE). Therefore, control of the ligand exchange process which efficiently substitutes the surface from long ligands to short molecules is necessary for CQD-based device applications.^{10,11} Enhanced performances of CQD solar cells using the inorganic halide ligands (e.g., Cl[−], Br[−], I[−]) have been recently reported,^{12,13} but the detailed characterization of the CQD film during the ligand exchange process has not been well investigated. Those parameters such as packing density or halide ion density on the surface should be considered for an effective way to control the surface status and further improve photovoltaic performance. Here, we investigate time-dependent influence of inorganic ligand exchange in lead sulfide (PbS) quantum dot films with systematic analysis of photovoltaic performance. Within the same concentration of tetrabutylammonium iodide (TBAI) which induces the same driving force of ligand exchange, we studied the charge transfer mechanism on quantum dot (QD) films based on the

quantitative interaction between surface halide ions and QD surface. Moreover, our study focused on the detailed status of the PbS surface for understanding the relationship between the packing density and charge carrier transport of PbS CQD films by adjusting ligand exchanging time. These findings will provide a useful guideline for achieving the high efficiency CQD-based solar cells.

Inorganic molecule halide treatment was carried out using TBAI solution in ambient conditions, which is one of the most commonly used ligand materials for PbS QD solar cells due to air-stability and low density of trapped carriers by highly effective passivation.^{12,13} During the ligand exchange, it introduces negatively charged iodine ions which substitute pristine oleic acid (OA). The halide anions subsequently bind to Pb cations on the PbS surface. If the surface is not perfectly upgraded, the remaining oleic acids will play a role as insulating barriers which decrease the carrier transport as well as exciton dissociation in PbS CQD films (Fig. 1(a)). Therefore, it is important to minimize the degree of the remaining oleic acids to improve the performance of photovoltaic devices by the controlled ligand exchange process, exposing the OA-capped CQD films to the solution containing the iodine ions. To systematically investigate the ligand exchanging effect, we prepared PbS CQD films with different ligand exchanging times (T_L): 15, 30, 60, and 90 s. 3 layers of PbS were deposited on glass substrates with TBAI solution (10 mg/ml in methanol). Evidence for chemical composition changes of the CQD surface can be determined using Fourier transform-infrared spectroscopy (FT-IR) and X-ray photoelectron spectroscopy (XPS) spectra of the iodide-treated PbS CQD films with the different ligand exchanging time of T_L . The presence of the oleic acids can be denoted by the four characteristic peaks including vibrations at 2920 cm^{−1} (asymmetric C-H), 2850 cm^{−1} (symmetric C-H), 1545 cm^{−1} (asymmetric COO[−]), and 1403 cm^{−1} (symmetric COO[−]), respectively. (Fig. 1(b)) Significant reduction of the OA-related vibrations was observed according to the treatment time.¹⁴ Together

^{a)}B.-S. Kim and J. Hong contributed equally to this work.

^{b)}Electronic addresses: junginn.sohn@eng.ox.ac.uk and seungnam.cha@eng.ox.ac.uk

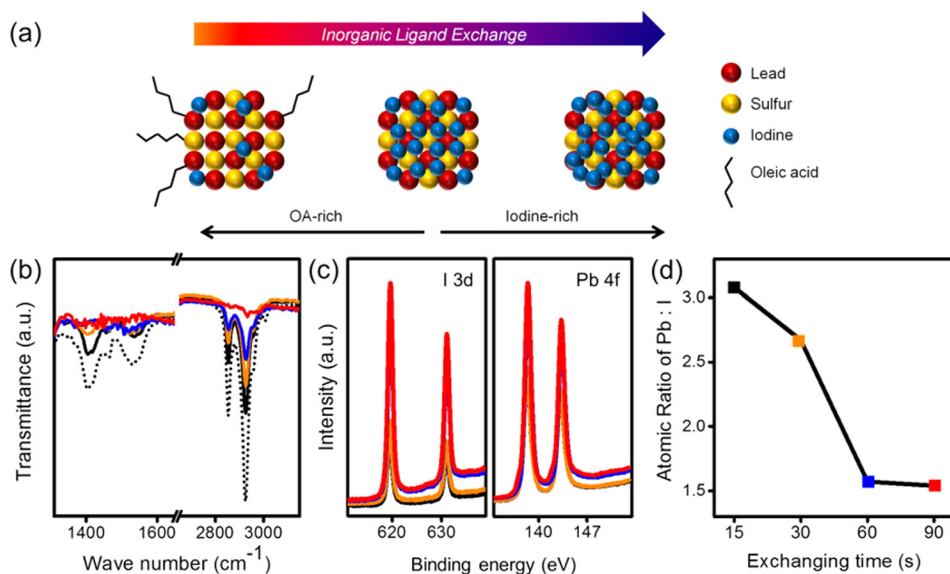


FIG. 1. A schematic illustrating the ligand exchange process on PbS CQD films. (b) FTIR spectra and (c) binding energy of I 3d and Pb 4f in TBAI-PbS CQD films with an increasing ligand exchanging time of T_L . They show successful exchange of iodine on the CQD surface. (d) Variation of the atomic ratio of lead to iodine as a function of the corresponding T_L . The squares and solid lines of black, orange, blue, and red are $T_L = 15, 30, 60$, and 90 s, respectively. The dotted lines in Fig. 1(b) are pristine PbS CQD film capping with oleic acid.

with the XPS energy spectra, the atomic ratios of lead and iodine on the surface of PbS CQD films can be evaluated with respect to the ligand exchanging time. Note that the short ligand exchanging time ($T_L < 30$ s) does not provide enough surface passivation and considerable oleic acids still remain on the PbS surface. With an increasing of T_L , the oleic acids were almost eliminated and surface iodine concentration is quantitatively increased. (Figs. 1(c) and 1(d)).

A degree of surface passivation could affect the morphological property of the PbS CQD film. Micro- and nano-scale cracks have been frequently observed in ligand-exchanged CQD devices due to the considerable volume shrink of the films when long oleic acids were substituted by short organic and/or inorganic ligands.^{15–17} Furthermore, the crack formation results in severe problems such as highly inducing short circuit or leakage current in CQD-based device applications.¹⁸ Therefore, careful control of the ligand exchange process is essential for producing crack-free CQD films. The morphological changes of the PbS CQD film were shown with the different ligand exchanging times of T_L (Fig. 2, Figs. S1 and S2

in [supplementary material](#)). A very rough surface with the numerous cracks was obtained at the T_L of 15 s while longer ligand exchanging time leads to a crack-free surface with the improved film flatness. This result implies that the presence of the residual oleic acids observed at insufficient ligand exchanging time induces the large physical strain with the coexistent short iodide ligands in PbS CQD films. It thus leads to the non-uniform volume shrink and accelerating crack formation during the solvent evaporation.

A highly densely packed CQD film is a critical factor to determine the photovoltaic performance since the charge carrier transport is enhanced with minimizing the CQD inter-particle distance.^{10,11} Figure 3 shows that the packing densities of the CQD film could be effectively tuned by adjusting the ligand exchanging time. Compared to OA-capped PbS CQDs, the packing densities were gradually increased with proceeding ligand exchange from OA to iodide molecules. (Figs. 3(a)–3(c)) Longer treatment makes the neighboring QDs closer, resulting in partially connection between each other. Furthermore, exciton absorption peaks were certainly

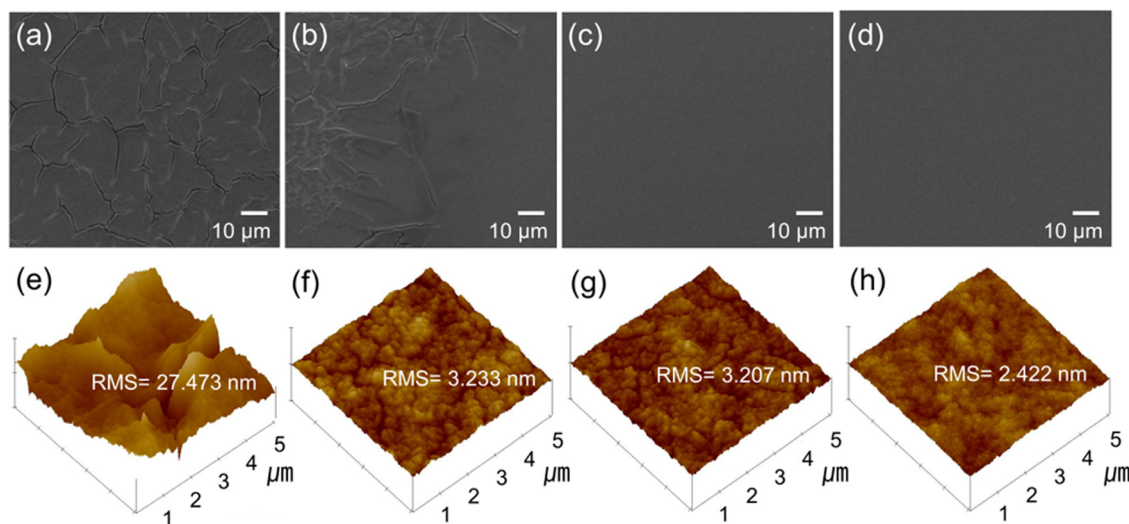


FIG. 2. Scanning electron microscopy (SEM) and atomic force microscopy (AFM) images of surface morphologies of TBAI-PbS films with increasing T_L : ((a) and (e)) 15 s, ((b) and (f)) 30 s, ((c) and (g)) 60 s, and ((d) and (h)) 90 s. These samples are prepared by spin coating the 3 layers of PbS onto the glass substrates. It was shown that the root mean square (RMS) roughness of PbS CQD films was gradually decreased, dependent on T_L .

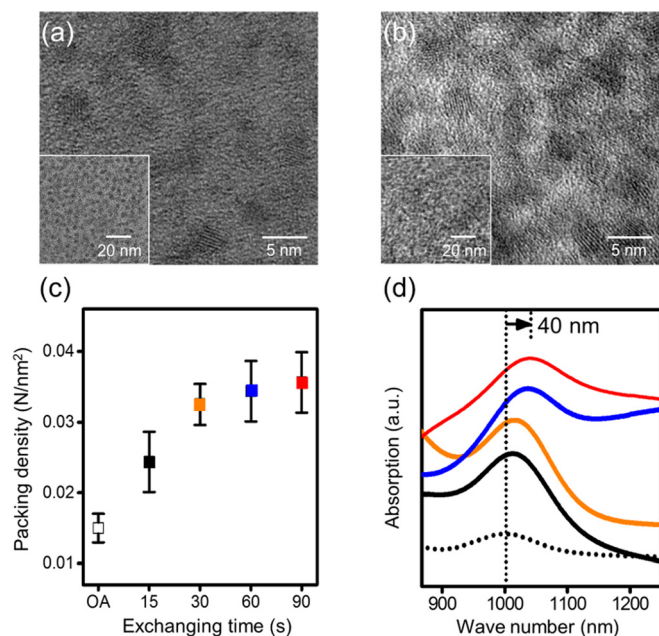


FIG. 3. Transmission electron microscopy (TEM) and selected area diffraction (SAED) pattern images of (a) pristine PbS CQD film capping with oleic acids and (b) TBAI-PbS CQD films at T_L of 30 s. With a longer time of 30 s, the packing density of the TBAI-PbS CQD film was slightly increased. Insets are low-magnification TEM images of the corresponding OA- and TBAI-PbS CQD films. (c) Variation of the packing density of PbS QDs as a function of T_L . (d) Absorption spectra of the corresponding PbS CQD films. The closed squares and solid lines of black, orange, blue, and red are $T_L = 15, 30, 60$, and 90 s, respectively. The open square and dotted line are pristine PbS CQD film capping with oleic acid.

observed to be broadened and red-shifted as seen in Fig. 3(d). These phenomena can be explained by electron coupling or sintering/necking between QDs as the inter-particle distance becomes closer.^{19–21} This correlates well with the increased packing densities with T_L observed by careful Transmission electron microscopy (TEM) analysis.

To investigate the relationship between photovoltaic performance of the PbS film with the different packing densities, we obtained photocurrent density and voltage (J - V) curves of the PbS CQD films with the different ligand exchanging times of T_L under AM 1.5G illumination (100 mW cm^{-2}). (Fig. 4(a)) The devices were prepared by 10 cycles spin coating of TBAI-PbS CQD films on ZnO/ITO substrates (Fig. S3 in [supplementary material](#)) and the photovoltaic performance of the devices is summarized in Figs. 4(c) and 4(d) (also see Fig. S4 in [supplementary material](#)). Incomplete passivation on the PbS surface caused by short ligand exchanging time of T_L hinders efficient charge transport in the film (Fig. 4(b)), resulting in relatively low short-circuit current (J_{sc}) and PCE with high series resistance (R_s). The device with a short T_L of 15 s gives a low PCE of 3.39% with a J_{sc} of 13.75 mA/cm^2 . Moreover, in Fig. S5, J_{sc} from the external quantum efficiency (EQE) measurement also shows the same trend which correlates with the J_{sc} enhancement of the J - V measurement by the different ligand exchanging times. With an increase of the ligand exchanging time, the packing densities of PbS QDs as well as surface coverage of the iodide molecule were significantly increased. (Figs. 1 and 3) It thus facilitates exciton dissociation via enhanced charge transfer in PbS films, leading to substantial improvement of 77.58% and 74.98% in PCE, and J_{sc} at T_L of 60 s, respectively (Fig. 4(c) and Table S1 in [supplementary material](#)). The values of R_s were also decreased from 10.14Ω to 3.51Ω , dependent on the T_L . Interestingly, we found that the photovoltaic performance was declined after longer T_L of 90 s in spite of the high surface coverage of iodide ligands on the PbS CQDs. It can be assumed that excess iodide molecules which are not bound to Pb cations may act as the insulating barrier between PbS CQDs. These results clearly indicate that the controlling ligand exchange on the PbS CQD film should be highly required to manipulate the photovoltaic performance.

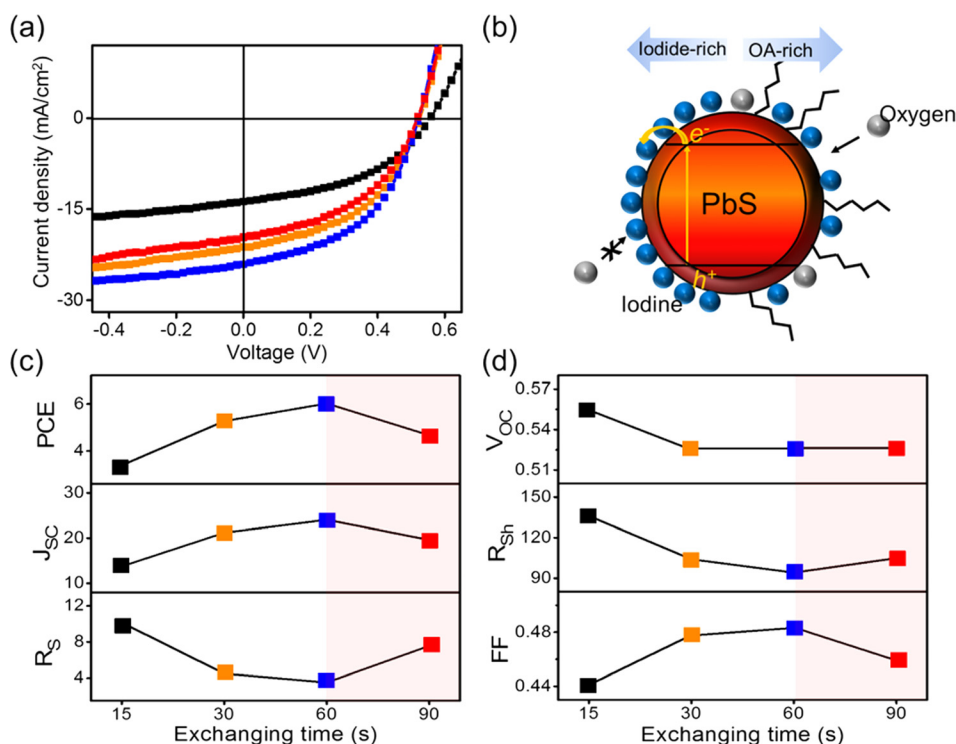


FIG. 4. (a) Representative J - V characteristics of the TBAI-PbS CQD devices by varying T_L . The devices were measured in the dark (open square) and under AM 1.5 illumination (close square) at an incident intensity of 100 mW/cm^2 . (b) Schematic of iodine- and OA-rich in PbS CQD. Plots of (c) PCE, J_{sc} , and R_s , (d) V_{oc} , R_{sh} , and fill factor (FF) of the devices as a function of T_L . The closed squares of black, orange, blue, and red indicate different T_L of 15, 30, 60, and 90 s, respectively.

We have demonstrated time-dependent inorganic ligand exchanging effect in PbS CQD films. Controlled surface passivation increases the packing density with a crack-free PbS surface by minimizing residual oleic acid. It also enables to facilitate charge transport and significantly improve PbS solar cell efficiency from 3.39% to 6.62%. Ligand exchange over a longer T_L of a critical value further decreases interparticle spacing but rather slightly deteriorates the photovoltaic performance by excess iodide molecules acting as a charge transport barrier on the PbS surface. These results distinctively prove that appropriate ligand passivation is highly required for high performance of the CQD solar cell.

See [supplementary material](#) for detailed growth procedures, supporting characterization, and analysis of nanomaterials.

The research leading to these results has received funding from the European Research Council under ERC Grant Agreement No. 340538. The authors would like to thank the financial support from the National Research Foundation (NRF) of Korea (2015M2A2A6A02045252). This work was conducted under the framework of Research and Development Program of the Korea Institute of Energy Research (KIER) (B6-2498).

¹A. P. Alivisatos, *Science* **271**(5251), 933 (1996).

²Z. Kang, Y. Liu, C. H. A. Tsang, D. D. Ma, X. Fan, N. B. Wong, and S. T. Lee, *Adv. Mater.* **21**(6), 661 (2009).

³D. A. Ruddy, J. C. Johnson, E. R. Smith, and N. R. Neale, *ACS Nano* **4**(12), 7459 (2010).

⁴L. Lu, J. Chen, and W. Wang, *Appl. Phys. Lett.* **103**, 123902 (2013).

⁵S. A. McDonald, G. Konstantatos, S. Zhang, P. W. Cyr, E. J. D. Klem, L. Levina, and E. H. Sargent, *Nat. Mater.* **4**(2), 138 (2005).

⁶X. Geng, L. Niu, Z. Xing, R. Song, G. Liu, M. Sun, G. Cheng, H. Zhong, Z. Liu, Z. Zhang, L. Sun, H. Xu, L. Lu, and L. Liu, *Adv. Mater.* **22**(5), 638 (2010).

⁷I. J. Kramer, G. Moreno-Bautista, J. C. Minor, D. Kopilovic, and E. H. Sargent, *Appl. Phys. Lett.* **105**(16), 163902 (2014).

⁸Z. Tan, J. Xu, C. Zhang, T. Zhu, F. Zhang, B. Hedrick, S. Pickering, J. Wu, H. Su, S. Gao, A. Y. Wang, B. Kimball, J. Ruzyllo, N. S. Dellas, and S. E. Mohny, *J. Appl. Phys.* **105**(3), 034312 (2009).

⁹C. B. Murray, C. R. Kagan, and M. G. Bawendi, *Annu. Rev. Mater. Sci.* **30**, 545 (2000).

¹⁰J. J. Choi, J. Luria, B. R. Hyun, A. C. Bartnik, L. Sun, Y. F. Lim, J. A. Marohn, F. W. Wise, and T. Hanrath, *Nano Lett.* **10**(5), 1805 (2010).

¹¹Y. Liu, M. Gibbs, J. Puthussery, S. Gaik, R. Ihly, H. W. Hillhouse, and M. Law, *Nano Lett.* **10**(5), 1960 (2010).

¹²C. H. M. Chuang, P. R. Brown, V. Bulović, and M. G. Bawendi, *Nat. Mater.* **13**(8), 796 (2014).

¹³Z. Ning, O. Voznyy, J. Pan, S. Hoogland, V. Adinolfi, J. Xu, M. Li, A. R. Kirmani, J. P. Sun, J. Minor, K. W. Kemp, H. Dong, L. Rollny, A. Labelle, G. Carey, B. Sutherland, I. Hill, A. Amassian, H. Liu, J. Tang, O. M. Bakr, and E. H. Sargent, *Nat. Mater.* **13**(8), 822 (2014).

¹⁴J. Tang, K. W. Kemp, S. Hoogland, K. S. Jeong, H. Liu, L. Levina, M. Furukawa, X. Wang, R. Debnath, D. Cha, K. W. Chou, A. Fischer, A. Amassian, J. B. Asbury, and E. H. Sargent, *Nat. Mater.* **10**(10), 765 (2011).

¹⁵M. H. Zarghami, Y. Liu, M. Gibbs, E. Gebremichael, C. Webster, and M. Law, *ACS Nano* **4**(4), 2475 (2010).

¹⁶J. M. Luther, M. Law, Q. Song, C. L. Perkins, M. C. Beard, and A. J. Nozik, *ACS Nano* **2**(2), 271 (2008).

¹⁷E. J. D. Klem, H. Shukla, S. Hinds, D. D. MacNeil, L. Levina, and E. H. Sargent, *Appl. Phys. Lett.* **92**(21), 212105 (2008).

¹⁸F. Hetsch, N. Zhao, S. V. Kershaw, and A. L. Rogach, *Mater. Today* **16**(9), 312 (2013).

¹⁹R. Koole, P. Liljeroth, C. De Mello Donegá, D. Vanmaekelbergh, and A. Meijerink, *J. Am. Chem. Soc.* **128**(32), 10436 (2006).

²⁰K. J. Williams, W. A. Tisdale, K. S. Leschkies, G. Haugstad, D. J. Norris, E. S. Aydil, and X. Y. Zhu, *ACS Nano* **3**(6), 1532 (2009).

²¹W. Ma, J. M. Luther, H. Zheng, Y. Wu, and A. P. Alivisatos, *Nano Lett.* **9**(4), 1699 (2009).